Discover Water

Research

Theoretical–experimental evaluation of the effects of Fe^{3+} ions in the disinfection of water supply by peracetic acid

Aline Karla Nolberto Souza[1] · Juliana Paggiaro[2] · Warlyton Silva Martins[3] · Anna Karla Santos Pereira[1] · Douglas Henrique Pereira[1] · Grasiele Soares Cavallini[1]

Received: 9 January 2024 / Accepted: 16 August 2024
Published online: 12 September 2024

Abstract
Peracetic acid (PAA) is efficient for disinfection processes in environmental sanitation and in the presence of transition metals its oxidative performance is enhanced. Thus, the present study aim evaluated the influence of Fe^{3+} ions during the inactivation process of *Escherichia coli* and Total Coliforms (TC). The process PAA + Fe^{3+} ions were also evaluated in relation to the disinfection kinetics, the participation of H_2O_2 and the influence of the organic load of the treated water. The tests showed an inactivation efficient of 0.5 to 0.9 log in relation to *E. coli* and 1.3 to 1.5 logs for TC in the concentrations evaluated and complete inactivation of *E. coli* was achieved within 15 min for both PAA and PAA/Fe^{3+} There is no damage to the disinfection process in the presence of Fe^{3+} ions, however, the decomposition of PAA is favored. In this sense, the formation of radicals can justify the maintenance of disinfection efficiency. The decay constants were close both microorganisms: for *E. coli* with PAA and PAA/Fe^{3+}were 0.0323 and 0.0476 and for TC were 0.0637 and 0.0667. The values of R^2 were above 0.95. Computer simulations of peptidoglycans that make up the bacterial cell wall showed that radicals preferentially attacked the carbons from the rings that composes the cell wall peptidoglycan of gram-negative bacteria allowing to break the structure during the disinfection process.

Keywords Radical formation · Disinfection · Water treatment · PAA · Fe^{3+}

1 Introduction

Peracetic acid (PAA) for environmental sanitation has been studied since 1980, and its advantages in relation to chlorinated disinfectants include a spectrum of similar sterilization, its oxygenation capacity, and the low number of toxic by-products [1]. In addition, several radicals can be formed using peracetic acid ($^{\bullet}OH$, $CH_3C(O)O^{\bullet}$, $CH_3C(O)^{\bullet}$, $CH_3C(O)OO^{\bullet}$, $^{\bullet}CH_3$, and/or $HO_2^{\bullet}$), which in turn can be combined with other compounds for the most efficient disinfection of water [2, 3]. Despite several studies focused on PAA-based AOPs for water and wastewater disinfection processes, it is still necessary to answer the exact mechanisms of PAA activation, the primary radical species involved, and the effectiveness of PAA-based AOPs in removing chemical and microbiological contaminants [1].

✉ Grasiele Soares Cavallini, grasiele@uft.edu.br; Aline Karla Nolberto Souza, alinenolberto@hotmail.com; Juliana Paggiaro, jupaggiaro@mail.uft.edu.br; Warlyton Silva Martins, warlytonsilva@gmail.com; Anna Karla Santos Pereira, anna_karla@uft.edu.br; Douglas Henrique Pereira, doug@uft.edu.br | [1]Graduate Program in Chemistry, Federal University of Tocantins, ZIP Code 77.402-970, Gurupi, TO, Brazil. [2]Graduate Program in Biotechnology, Federal University of Tocantins, 77.402-970, Gurupi, TO, Brazil. [3]Graduate Program in Plant Production, Federal University of Tocantins, 77.402-970, Gurupi, TO, Brazil.

The rapid decomposition of PAA has been described as a disadvantage, but recent studies have shown that this decomposition results in radicals that are important to the oxidative process, such as alkoxyl radicals ($RO^{\bullet}$), organic peroxyl ($ROO^{\bullet}$), and singlet oxygen ($^1O_2$) [4–6]. This information is relevant because it elucidates the mechanism of PAA decomposition, which in the past was described simply as the formation of acetic acid and oxygen [7] [8], without considering the possible formation of chemical species relevant to the disinfection process, particularly in the presence of catalysts such as iron [4].

Although the degradation mechanisms of PAA have been reported for several decades [9], the detailed mechanism of PAA – iron is still under debate and has taken a recent interest within the AOP research field [10]. The use of the combination of PAA/Fe(II, III) rather than classical Fenton (H_2O_2/Fe(II, III)) or persulfate/Fe(II, III) is more convenient due faster reaction of PAA reacts with Fe(II) compared with H_2O_2 and its coexistent H_2O_2 [10]. PAA activated by iron-based materials can generate more selective radicals, such as $CH_3C(O)O^{\bullet}$ and $CH_3C(O)OO^{\bullet}$, which are little explored/applied for environmental systems despite their potential [11]. Additionally, Fe (II) is an environmentally benign metal that is naturally present in soil and water [10].

Studies have shown that the combination of PAA/$FeCl_3$ can promote faster degradation/oxidation processes because it is a system with thermodynamically spontaneous reactions [4]. Furthermore, the peroxide bond energy of PAA is much lower than that of H_2O_2 used in the classical Fenton process, which facilitates oxidation and the production of more oxidative specie [12]. However, verification of this combination for the disinfection process has not yet been reported in the literature; therefore, the present study evaluated the combination of PAA and Fe^{3+} ions for water disinfection, using *E. coli* as a bioindicator of contamination as well as total coliforms. Together with the experimental results, computational simulations at the density functional theory (DFT) level were performed in the peptidoglycan structure of bacteria cell walls to evaluate the possible sites of radical attacks to understand how the breakdown of structures and the inactivation of microorganisms occur.

In this sense, research carried out in a natural source of water that supplies the city of Gurupi in the state of Tocantins – Brazil (Água Franca Stream) presents the integration of theoretical and experimental approaches for a comprehensive understanding of the combination of PAA/$FeCl_3$ for the disinfection process, offering new solutions or optimizations for water treatment plants.

2 Materials and methods

2.1 Materials

The reagents ferric chloride hexahydrate (p.a.), 15% commercial PAA solution (containing 15% PAA, 23% hydrogen peroxide, 16% acetic acid, and 46% water (w/w)) adquired from Tech Desinfecção, 35% solution of hydrogen peroxide (p.a.), Agar Chromocult® Coliformes from Merck and N, N-diethyl-p-phenylenediamine (DPD) Chemetrics® were used. Residual PAA was measured on a T60 UV–visible spectrophotometer (PG).

Water samples were collected from the Água Franca Stream in Gurupi (11°44′30″ S 49°02′30″ W) from April to September 2021. Crude water samples were collected on the same days as that of the experiment. After sample collection, raw water was characterized physicochemically by the parameters of pH, biochemical oxygen demand (BOD), total solids, turbidity, and absorbance at 254 nm, and microbiologically from *E. coli* and total coliform (TC) counts using the filter membranes method [13]. The characterization of the samples with their maximum and minimum values for each parameter is presented in Table 1.

2.2 Inactivation of E. coli and TC by different concentrations of *PAA*/$FeCl_3$ at different contact times

Different concentrations of PAA and $FeCl_3$ were evaluated at various contact times, as shown in Table 2. Eight trials resulting from eight collections were performed, with each collection performed on a different day.

For the disinfection tests, 300 mL of samples (river water) were used, which were placed in a beaker and kept under constant stirring on a magnetic stirrer during the disinfection process. Contact time was interrupted with the addition of three drops of sodium thiossulfate ($Na_2S_2O_3$) at 1%. The determination of residual PAA was performed by the spectrophotometric method at 530 nm using the reagent N, N-diethyl-p-phenylenediamine (DPD) Chemetrics®.

Table 1 Physicochemical and microbiological characterization of raw water

Parameter	Maximum and minimum value
pH	6.8–7.87
Turbidity (NTU)	12–23.3
Abs_{254nm}	0.071–0.092
E. coli (CFU.100 mL^{-1})	120–3000
Total Coliforms (CFU.100 mL^{-1})	1200–11400
BOD_5 ($mg.L^{-1}$)	4
Conductivity (μScm^{-1})	15.21–49.74

Table 2 Sequence of inactivation tests of *E. coli* and Total Coliforms

Assay	[PAA]	[Fe^{3+}]	Contact time (min)
01	13 $\mu mol.L^{-1}$	0	5, 15 e 30
		10 $\mu mol.L^{-1}$	
02	13 $\mu mol.L^{-1}$	0	5 e 10
		1 $\mu mol.L^{-1}$	
		3 $\mu mol.L^{-1}$	
		5 $\mu mol.L^{-1}$	
03	13 $\mu mol.L^{-1}$	0	1,5,10,15 e 20
		5 $\mu mol.L^{-1}$	
04	26 $\mu mol.L^{-1}$	0	5,10,15 e 20
		5 $\mu mol.L^{-1}$	
		10 $\mu mol.L^{-1}$	
05	39 $\mu mol.L^{-1}$	0	5,10, 15 e 20
		15 $\mu mol.L^{-1}$	
	65 $\mu mol.L^{-1}$	0	
		25 $\mu mol.L^{-1}$	
06	130 $\mu mol.L^{-1}$	0	5,10, 15 e 20
		50 $\mu mol.L^{-1}$	
		75 $\mu mol.L^{-1}$	
	195 $\mu mol.L^{-1}$	0	
07	65 $\mu mol.L^{-1}$	0	20
		25 $\mu mol.L^{-1}$	
	130 $\mu mol.L^{-1}$	0	
		50 $\mu mol.L^{-1}$	
	195 $\mu mol.L^{-1}$	0	
		25 $\mu mol.L^{-1}$	
		37.5 $\mu mol.L^{-1}$	
		75 $\mu mol.L^{-1}$	
	260 $\mu mol.L^{-1}$	0	
		37.5 $\mu mol.L^{-1}$	
		50 $\mu mol.L^{-1}$	
		100 $\mu mol.L^{-1}$	
	390 $\mu mol.L^{-1}$	50 $\mu mol.L^{-1}$	
		75 $\mu mol.L^{-1}$	
		150 $\mu mol.L^{-1}$	
08	13 $\mu mol.L^{-1}$	5 $\mu mol.L^{-1}$	1440

2.3 Microbiological evaluation

After the disinfection tests, the treated water samples were filtered through a vacuum filtration system using a sterile checkered cellulose nitrate membrane with a porosity of 0.45 µm and 47 mm in diameter. After the filtration process, the membranes were inserted into Petri dishes containing specific culture medium (selective and differential) for fecal coliforms (Chromocult® Coliformes Agar, Merck) and incubated at 36 °C for 24 h. After this time, the colonies formed in Colony Forming Units per 100 mL (CFU.100 mL^{-1}) were counted. When necessary, the samples were fractionally diluted in sterile water [13]. The tests were performed in triplicate, with each container containing 300 mL of sample, with 100 mL being filtered at a time.

2.4 Determination of the decay constant

For the kinetic study, the PAA and PAA/Fe^{3+} processes were evaluated, using concentrations of 13 µmol.L^{-1} PAA and 5 µmol.L^{-1} Fe^{3+} at 10, 15, and 20 min. For determination of the decay constant (k), Chick's law was used [14]. This law is applied to constant concentrations of disinfectant over time, and the disinfection constant (k) is the angular coefficient of the line equation obtained by the ln (N/N_0) and time (in minutes) by linear regression. As there is no possibility of increasing the initial concentration, the intersection of the line on the y-axis should be zero [15].

2.5 Evaluation of the contribution of hydrogen peroxide (H_2O_2) to disinfection with *PAA* and *PAA*/Fe^{3+}

This assay was conducted considering the concentration of H_2O_2 contained in the 13 µmol L^{-1} PAA solution, which was 45 µmol.L^{-1}, due to the quaternary composition of commercial PAA (15% PAA + 23% H_2O_2 + 16% acetic acid + water). The disinfection assay was used to evaluate the isolated effect of H_2O_2 in the sample and the H_2O_2/Fe^{3+} combination. Concentrations evaluated were: H_2O_2 (45 µmol.L^{-1}), the combination with H_2O_2 (45 µmol.L^{-1}), and Fe^{3+} (5 µmol.L^{-1}). The contact times evaluated were 10 and 20 min.

2.6 Computational simulations

To evaluate the attack of radicals on the cell wall, a peptidoglycan structure was simulated and the molecular electrostatic potential (MEP), frontier molecular orbitals (FMO) analysis, and Fukui reactivity indices were determined.

The structures were optimized to the minimum energy using density functional theory (DFT) with functional B3LYP [16–19] and basis set 6-31G (d,p) [20–22]. To confirm that the optimized structure was at its minimum energy, a frequency calculation was employed and no imaginary frequency was found. The effect of water as a solvent was investigated using the continuous solvent model SMD [23].

The DFT can be predicted nucleophilic, electrophilic and radical attacks through Fukui indices. The condensed version of the Fukui function for a radical attack can be calculated using Eq. 1 [24]:

$$Radicalattack : \left(f_k^0 = \left(q_{(N-1)}^k - q_{(N+1)}^k\right)\right)\Big/2 \quad (1)$$

where q_{N+1}^k and q_{N-1}^k are the charges of the molecules in their anionic and cationic forms, respectively. The atomic charges calculated and used to determine radical attacks were natural population analyses (NPA) [25].

All calculations were performed using the Gaussian 09 program [26] and some structures were visualized using the GaussView program [27].

Table 3 Inactivation of *E. coli* and TC, using 13 µmol.L^{-1} PAA and 10 µmol.L^{-1} Fe^{3+}, at different contact times

Contact time (min)	PAA/Fe^{3+}		PAA	
	E. coli (CFU.100 mL^{-1})	TC (CFU.100 mL^{-1})	*E. coli* (CFU.100 mL^{-1})	TC (CFU.100 mL^{-1})
0	1200	10,000	1200	10,000
5	184	600	343	735
15	1	63	1	70
30	1	54	1	68

3 Results and discussion

3.1 Tests with different concentrations of *PAA* and *PAA*/Fe^{3+} with varying contact times

The preliminary test to evaluate the combined effect of PAA and Fe^{3+} was performed using the proportions of the reagents proposed by [4], which were close to 1:1. After 15 min of contact, the inactivation *of E. coli* was complete, both for PAA and for PAA/Fe^{3+}. The CFU counts was performed and results are shown in Table 3.

Table 3 shows that at 5 min, the inactivation efficiency for *E. coli* and Total coliforms (TC) was greater with the use of PAA/Fe^{3+}, highlighting the potential of this combination. These results were used to determine the ideal time for achieving good, but not complete, inactivation, which is crucial for evaluating the effects of varying oxidant/catalyst concentrations. The time of 5 min and 10 min were fixed to observe differences in efficiencies without achieving complete inactivation and different concentrations of PAA and Fe^{3+} were evaluated to establish the proportion between the oxidant and the catalyst, as shown in Fig. 1.

There was no difference in the efficiency of TC inactivation, even with increased contact time and Fe^{3+}concentrations. For *E. coli*, the difference was 0.1 log. Assays with higher PAA concentrations were evaluated aimed to maintain a sufficient level of oxidant to achieve effective disinfection. This strategy can to ensure availability of the oxidant until the end of the disinfection process. Thus, the PAA concentration evaluated was 26 µmol.L^{-1} with Fe^{3+} concentrations of 5 µmol.L^{-1} and 10 µmol.L^{-1}, to create trials in the proportions of PAA/Fe^{3+} of 5:1 and 2.6:1, respectively (Fig. 2) and assays with PAA concentrations of 39 µmol.L^{-1} and 65 µmol.L^{-1} were evaluated, with PAA/Fe^{3+} proportions of 8:1 and 2.6:1 (Fig. 3), both at 15 and 20 min of contact time.

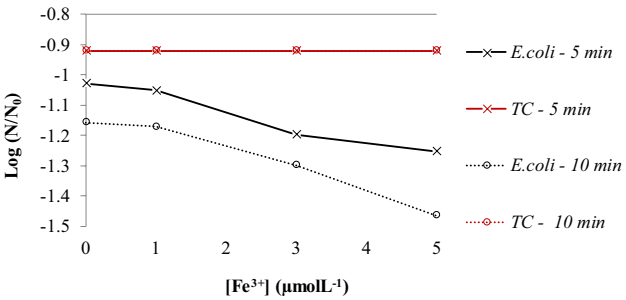

Fig. 1 Inactivation of *E. coli and* TC, at 13 µmol.L^{-1} PAA and variable concentrations of Fe^{3+}, in contact time of 5 min and 10 min

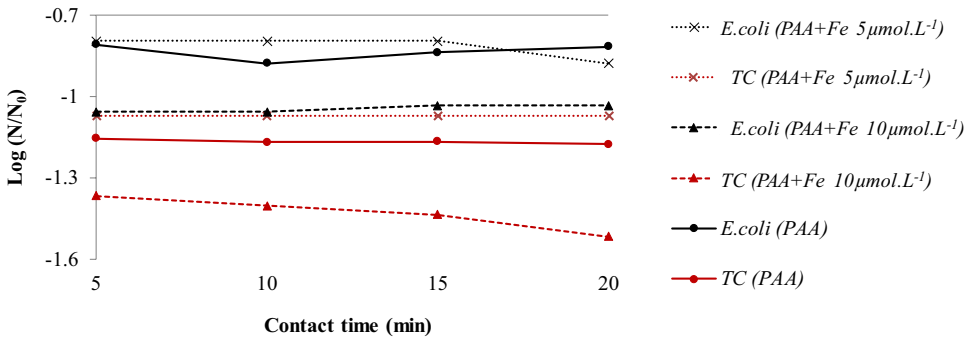

Fig. 2 Inactivation of *E. coli* and TC, using 26 µmol.L^{-1} PAA and concentrations Fe^{3+} of 5 and 10 µmol.L^{-1}, with contact times of 5 to 20 min

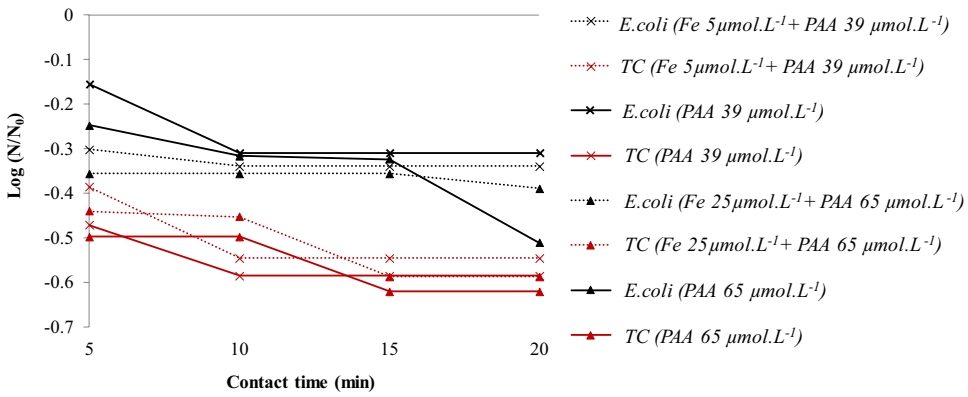

Fig. 3 Inactivation of *E. coli* and TC, in concentrations of PAA at 39 and 65 µmol.L^{-1} and concentrations of Fe^{3+} at 5 and 25 µmol.L^{-1} with contact time of 5 to 20 min

Table 4 Physical–chemical and microbiological characterization of water

Parameter	Maximum and minimum value
pH	6.8–6.9
Turbidity (NTU)	11–13
Abs_{254nm}	0.130–0.176
BOD_5 (mg.L^{-1})	10
E. coli (CFU.100 mL^{-1})	150–450
Total Coliforms (CFU.100 mL^{-1})	3000–8000

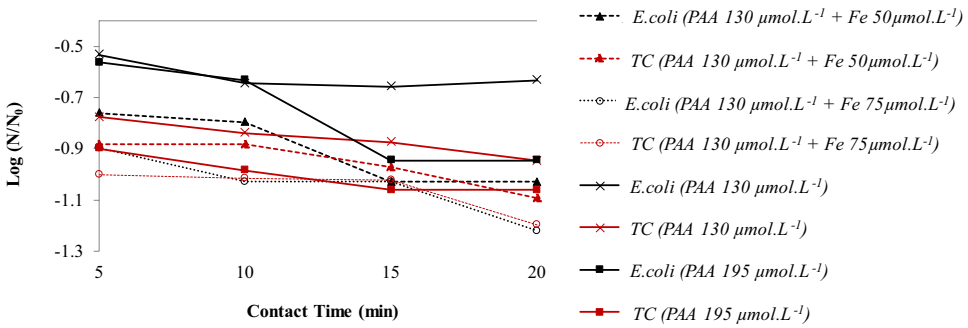

Fig. 4 Inactivation of *E. coli* and TC, in PAA concentrations at 130 µmol.L^{-1} and Fe^{3+} concentrations at 50 and 75 µmol.L^{-1}, with a contact time of 5 to 20 min

Regarding the of *E. coli* inactivation values at 10 and 15 min, the treatments presented similar values (from 0.25 to 0.5 log). For total coliforms, the difference was 0.1 log. The spontaneous decomposition of PAA generates acetic acid and oxygen [8], in the presence of Fe(III) ions the decomposition is catalyzed [4]. In some elementary steps of the mechanism, radicals are formed, which are capable of oxidizing organic matter [28]. Therefore, the decrease in disinfection efficiency was not observed. It is worth noting that the addition of iron ions can be recommended for this purpose, however, for disinfection, although there is no harm, the significant increase in efficiency was not achieved.

3.2 Disinfection assays with higher organic matter content

The raw water characteristics in this test are shown in Table 4.

Even using a ten times higher concentration of PAA, the inactivation efficiencies remained low. Figure 4 shows the results obtained.

Using a 3 times higher dosage of PAA (390 µmol.L^{-1}), compared to the previous assay, the efficiencies did not increase and remained varying from 0.5 to 0.9 log in relation to *E. coli* and 1.3 to 1.5 logs for TC. Figure 5 show the inactivation results for *E. coli* and TC, respectively.

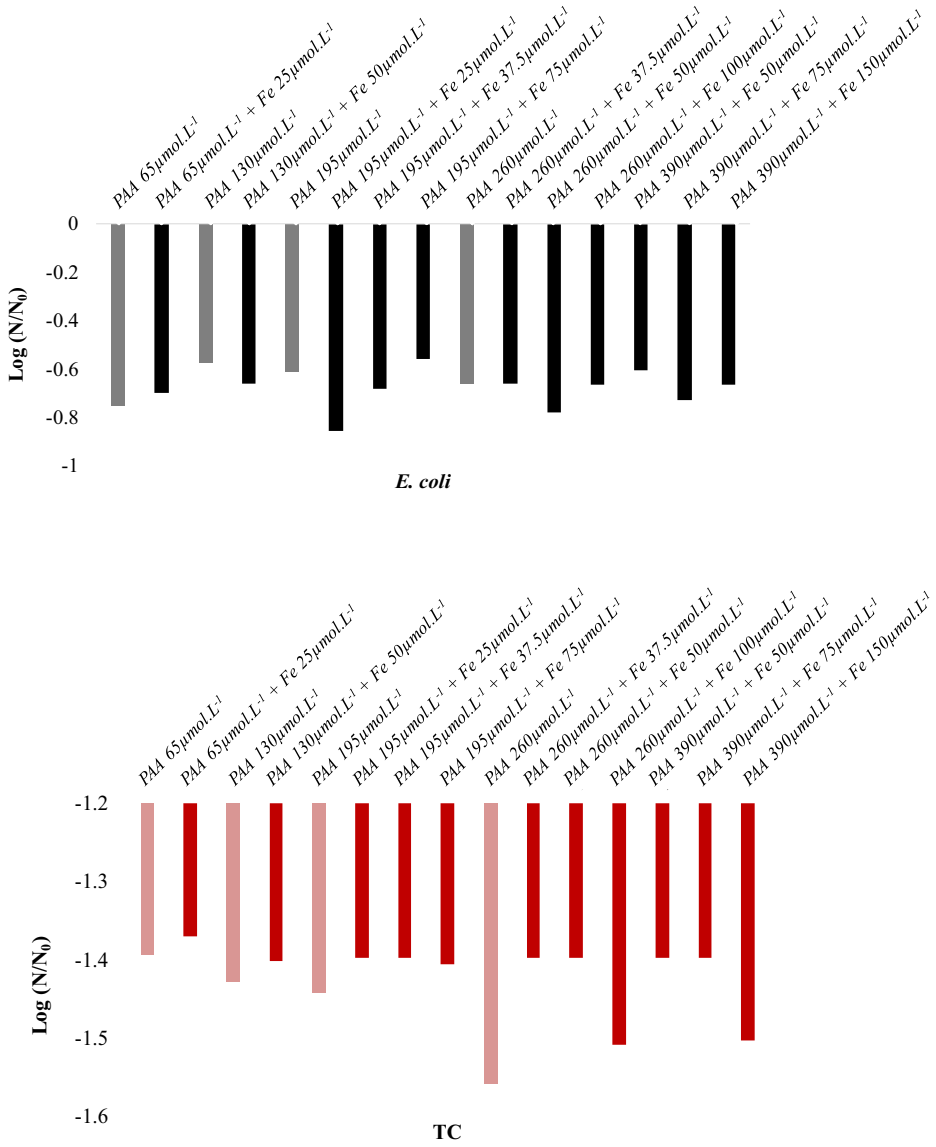

Fig. 5 Inactivation of *E. coli* and Total Coliform, in PAA concentrations between 65 and 390 μmol.L^{-1} and Fe^{3+} concentrations between 25 and 150 μmol.L^{-1}, with a contact time of 20 min

It can be observed, in Fig. 5, an increase in the efficiency of inactivation of *E. coli* in the presence of Fe^{3+} ions. However, the combined process showed lower inactivation efficiency compared to total coliforms.

Regarding the increase in PAA concentration, it can be observed that even maintaining the proportion of PAA/Fe^{3+} from 2 to 3:1, the increase in inactivation was not achieved with the excess of the oxidant, showing that the increase in organic matter interferes in the action PAA/Fe^{3+} disinfectant. This happens because the reactive oxygen species that promote disinfection are not selective. That is, it will react with any organic matter present in the medium. According to Ksibi (2006) both hydrogen peroxide and PAA promote disinfection through the oxidation of intracellular components of organisms, but may have low inactivation due to pollutants or high concentration of organic matter in the medium.

3.3 Kinetic study of disinfection with *PAA* and *PAA*/Fe^{3+}

Disinfection kinetics were determined for the PAA and PAA/Fe^{3+} processes using a PAA concentration of 13 μmol.L^{-1} and Fe^{3+} of 5 μmol.L^{-1}, at 10, 15, and 20 min, as shown in Fig. 6.

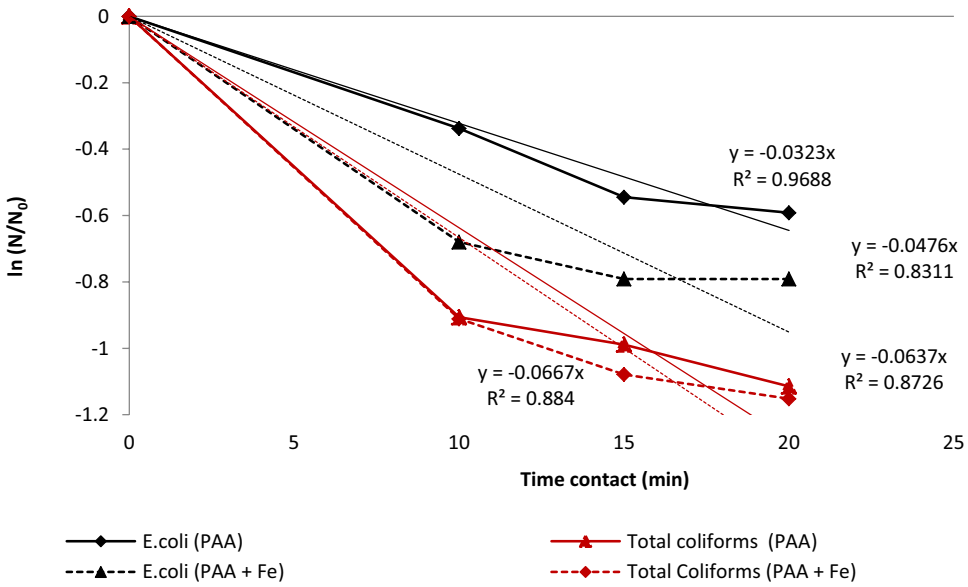

Fig. 6 Study of the kinetics of disinfection of *E. coli and* Total Coliforms using PAA (13 µmol. L^{-1}) and PAA/Fe^{3+} (13 µmol. L^{-1}/5 µmol. $L.^{-1}$)

Table 5 Physicochemical characterization after kinetic disinfection assays

Parameters[a]	Raw Water	PAA assay	PAA/Fe^{3+} assay
pH	7.22	7.01	6.08
Conductivity (µSm^{-1})	15.21	16.23	19.35
Residual PAA (µmol.L^{-1})	–	9.23	8.19
Dissolved oxygen (DO) (mg.L^{-1})	6.79	7.05	6.89
BOD_5 (mg.L^{-1})	10	8	9

[a]Samples evaluated at contact time of 20 min

Figure 6 shows that the values of the *E. coli* disinfection constant with PAA and PAA/Fe^{3+} were 0.0323 and 0.0476, respectively, while total coliforms with PAA and PAA/Fe^{3+} were respectively, 0.0637 and 0.0667. As the line indicates the decline in the number of microorganisms, the value of the angular coefficient is negative.

According to Daniel et al. (2001), the decay constant (k) increases with increasing disinfectant concentration, resulting in higher inactivation efficiency. Although the PAA/Fe^{3+} process was faster the difference between the values were too low to indicate a significant increase in speed. It is also noted that the value of R^2 was above 0.95 for all trials.

Table 5 presents the physicochemical parameters evaluated after the disinfection processes with PAA (13 µmol.L^{-1}) and PAA/Fe^{3+} (13 µmol.L^{-1}/5 µmol.L^{-1}).

Considering the residual values of PAA (Table 5), a higher consumption of the oxidant in the PAA/Fe^{3+} process was observed, and the maintenance of the inactivation efficiency. In the presence of metal ions, a greater decomposition of PAA was expected, which would imply a reduction in the inactivation process, but this was not observed. In this case, the Fe^{3+} ions catalyzed the formation of radicals, which can act as disinfectants.

There was no increase in the BOD of the samples with the addition of PAA, which can be explained by the release of molecular oxygen during the five days of analysis, resulting from the decomposition of H_2O_2 and CH_3COOOH from commercial PAA. Regarding the DO parameter, the concentrations of dissolved oxygen in the samples were similar, even in the samples with the addition of PAA, which demonstrates that the release of oxygen was slow and undetected in the first hour of the reaction.

The acidification capacity of the sample by PAA was lower than that of the salt chloric chloride at concentrations of 13 µmol.L^{-1} PAA and 5 µmol L^{-1} Fe^{3+}. The increase in conductivity occurred due to the increase in dissolved PAA and iron chloride ions.

Table 6 Evaluation of the contribution of hydrogen peroxide in disinfection with PAA and PAA/Fe^{3+}

(CFU.100 mL^{-1})	Tests with H_2O_2	10 min	20 min	Tests with PAA	10 min	20 min
E. coli	H_2O_2	240	180	PAA	112	94
Total Coliforms		1100	1000		800	800
E. coli	H_2O_2/Fe^{3+}	222	202	PAA/Fe^{3+}	70	76
Total coliforms		800	800		400	400
E. coli	Raw water	700				
Total Coliforms		4800				

Table 7 Inactivation of *E. coli and* TC for a prolonged period

(CFU.100mL^{-1})	After disinfection		24h after disinfection	
	PAA/Fe^{3+}	What	PAA/Fe^{3+}	What
E.coli	78	83	02	09
Total coliforms	158	164	57	92

3.4 Contributions of hydrogen peroxide to disinfection

Hydrogen peroxide assays in the presence and absence of Fe^{3+} were performed under the same conditions as the PAA and PAA/Fe^{3+} assays to compare the effects on water disinfection (Table 6). The concentration of hydrogen peroxide was the same as that contained in the 13 µmol.L^{-1} PAA solution (45 µmol.L^{-1} of H_2O_2).

In this assay, hydrogen peroxide contributed to the disinfection process. This behavior was expected considering that the iron ions allowed the formation of radicals that aid in the disinfection process, both with the use of hydrogen peroxide and organic peroxides such as PAA [4, 29]. Notably, in relation to the inactivation *of E. coli, the* combined process (H_2O_2/Fe^{3+}) did not show significant differences compared to the assay with H_2O_2 without Fe^{3+}.

3.5 Evaluation of disinfection by *PAA* and *PAA*/Fe^{3+} processes with prolonged contact times

Disinfection at prolonged contact times was evaluated at concentrations of 13 µmol.L^{-1}PAA and 5 µmol.L^{-1} Fe^{3+}, and the results are shown in Table 7.

According to Table 7, as the contact time increased, the difference between disinfection processes was clearer, as shown in Fig. 7.

3.6 Computational simulations

Through theoretical chemistry it is possible to understand why even with the decomposition of PAA by Fe^{3+} ions, the disinfection process is not compromised. Theoretical studies were conducted to elucidate the possible sites of attack by radicals using a peptidoglycan molecule. This polymer exists in the cell walls of gram-positive and gram-negative bacteria and forms a mesh-like layer; therefore, it is formed on the outside of the cytoplasmic membrane [30]. In this context, the presents study was based on the arrangement described by Vollmer and Bertsche (2008), using the peptidoglycan of gram-negative bacteria (*E. coli*) and aims to identify possible sites that may be attacked by radicals. For the computational simulations, a cut was made in the polymer, and the structure evaluated contained three rings: 1, 6-anhydroMurNac, GlcNAc, and MurNAc. The molecular structure, the MEP, FMO and Fukui indices results are represented in Fig. 8. The ends of the cuts were supplemented with hydrogen according to similar polymer simulation methodologies [31–34].

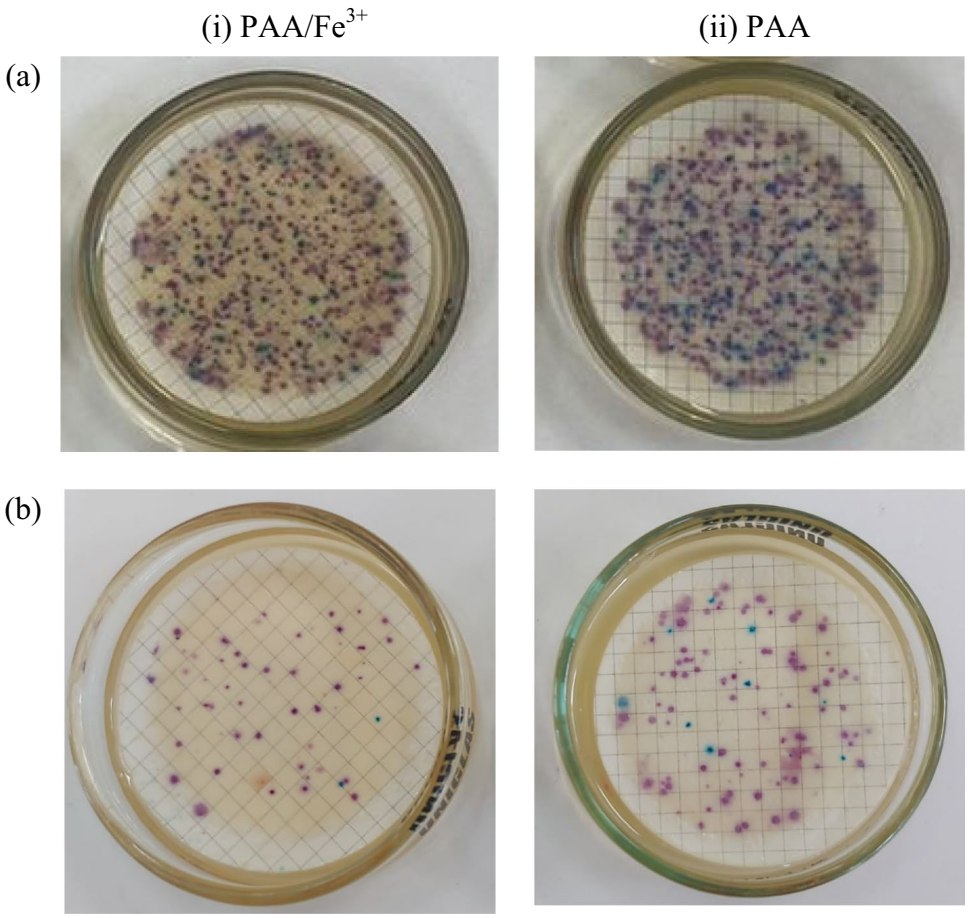

Fig. 7 Inactivation of *E. coli* and TC after disinfection **a** with contact time of 20 min and **b** with contact time of 24 h

Analyzing the FMOs, (Fig. 8b) it was possible to observe that the HOMO had a well-defined π format in the 1, 6-anhydroMurNac and GlcNAc residues. The LUMO also had a π format only at the termination of the MurNAc residue. The location of orbitals can provide important information about the chemical reactivity that occurs through the FMOs [35].

The points of greatest reactivity of the molecule can be observed through the MEP in the regions of more intense colors, in which blue indicates a partially positive region and the more orange or shades of red are partially negative regions (Fig. 8c). Anions or radicals appeared to interact with the positive part of the N-acetylmuramic group (MurNAc) that contain positive hydrogen atoms. The negative regions are located on the oxygen and nitrogen atoms, resulting from the pair of electrons isolated from these atoms, which suggests that these regions may interact with cations.

Fukui reactivity indices are used to predict nucleophile, electrophilic, and radical attack reactivity sites and are represented in Fig. 8d. Only the optimal sites for radical attack were represented, and the higher the values of f^0, the more reactive the site was for radical attack. Analyzing the results for the Fukui index, it is possible to observe that the generated radicals can attack some carbons from three rings that make up the cell wall of a gran negative bacteria, proving that the radicals can oxidize the cell wall and thus inactivate the bacteria by DFT simulation. These results allow to explain the indirect exogenous mechanisms [36–40].

4 Conclusions

It can be concluded that Fe^{3+} ions do not harm to the process of disinfection with PAA, both in the inactivation efficiency of *E. coli* and total coliforms and disinfection kinetic.

Predominantly the disinfection process with PAA/Fe^{3+} demonstrated superior efficiencies, however, they were not enough for the addition of Fe^{3+} ions to be recommended to accelerate or increase the disinfection capacity. However,

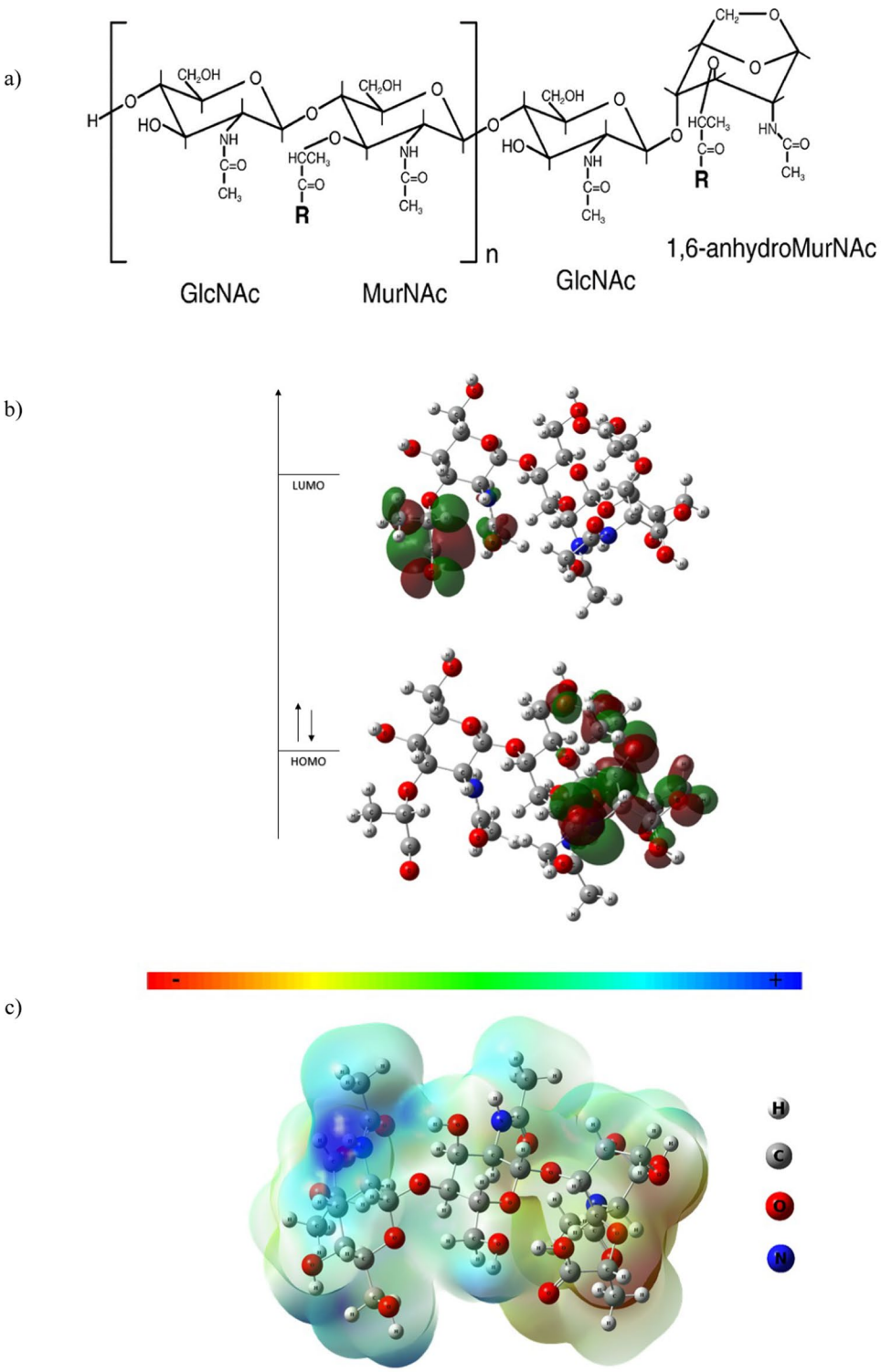

Fig. 8 **a** Molecular structure, **b** Frontier Molecular Orbitals, **c** molecular electrostatic potential and **d** Fukui indices for radical attacks (f^0) for peptideoglycan polymer

Fig. 8 (continued)

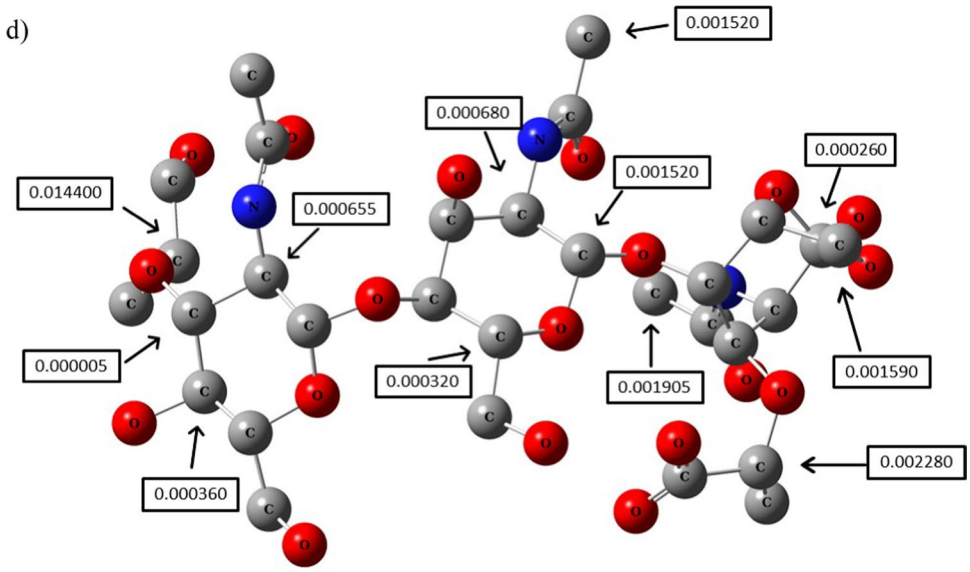

when PAA was used in excess, the contribution of Fe^{3+} ions could not be detected, because disinfection occurs mainly by PAA and not by radicals.

Water with a high content of organic matter significantly affects disinfection processes with PAA and PAA/Fe^{3+} and compromises the process of microorganism inactivation.

In relation to the PAA residual, the PAA/Fe^{3+} process presented an oxidant consumption higher than that of the PAA process, which can be attributed to the decomposition of PAA in the presence of Fe^{3+} ions for the formation of radicals when there was greater inactivation.

Hydrogen peroxide contributed to the disinfection processes with PAA and PAA/Fe^{3+}; however, it was less influenced by Fe^{3+} ions.

The results of the simulations show that the generated radicals can remove hydrogen from the cell wall or interact with ions as described by MEP and FMOs. The Fukui indices showed that some carbons from three rings probably will interact with the radicals disrupting the cell wall.

In general, it is important to highlight that the results presented in this study contribute to a greater understanding of the possibility of the formation of radicals from the decomposition of PAA in the presence of Fe^{3+} ions, demonstrating that, under these conditions, the decomposition of PAA favors the disinfection process and Fe^{3+} acts as a catalyst and not an interference.

Author contributions A.K.N.S.: Methodology, Investigation, Writing – Original Draft; J.P. and W.S.M.: Investigation; A.K.S.P, D.H.P. and G.S.C.: Conceptualization, Supervision, Writing – Review & Editing.

Funding This research was funded by PDPG-POSDOC (Programa de Desenvolvimento da Pós-Graduação (PDPG) Pós-Doutorado Estratégico—Postgraduate Development Program (PGDP) Strategic Postdoctoral) No. 88887.798251/2022–00. This work was supported by CAPES (Coordination of Improvement of Higher Education Personnel, Brazil, Funding Code 001 CAPES) and the PROPESQ/Federal University of Tocantins (Edital para tradução de artigos científicios da Universidade Federal do Tocantins, PROPESQ/UFT). Pereira D.H. acknowledges the Center for Computational Engineering and Sciences (Financial support from FAPESP Fundação de Amparo à Pesquisa, Grant 2013/08293–7, and Grant 2017/11485–6) and the National Center for High Performance Processing (Centro Nacional de Processamento de Alto Desempenho – CENPAAD) in São Paulo for computational resources. The authors thank the Tocantins Research Support Foundation—FAPT for the financial support. The authors thank the Thech Desifecção Ltda.

Data availability The datasets generated during and/or analysed during the current study are available from the corresponding author on reasonable request.

Declarations

Competing interests The authors declare no competing interests.

References

1. Ao X, Eloranta J, Huang C-H, Santoro D, Sun W, Lu Z, et al. Peracetic acid-based advanced oxidation processes for decontamination and disinfection of water: a review. Water Res. 2021;188: 116479. https://doi.org/10.1016/j.watres.2020.116479.
2. Aguiar A, Ferraz A, Contreras D, Rodríguez J. Mecanismo e aplicações da reação de fenton assistida por compostos fenólicos redutores de ferro. Quim Nova. 2007;30:623–8. https://doi.org/10.1590/S0100-40422007000300023.
3. Bezerra LB, Carlos TD, Nogueira Neves AP, Duraes WA, de Almeida SR, Pereira DH, et al. Theoretical-experimental study of the advanced oxidative process using peracetic acid and solar radiation: Removal efficiency and thermodynamic elucidation of radical formation processes. J Photochem Photobiol A Chem. 2022;423:113615. https://doi.org/10.1016/j.jphotochem.2021.113615.
4. Carlos TD, Bezerra LB, Vieira MM, Sarmento RA, Pereira DH, Cavallini GS. Fenton-type process using peracetic acid: Efficiency, reaction elucidations and ecotoxicity. J Hazard Mater. 2021;403: 123949. https://doi.org/10.1016/j.jhazmat.2020.123949.
5. Kim J, Wang J, Ashley DC, Sharma VK, Huang C-H. Enhanced degradation of micropollutants in a peracetic acid–Fe(III) system with picolinic acid. Environ Sci Technol. 2022;56:4437–46. https://doi.org/10.1021/acs.est.1c08311.
6. Kotowska U, Karpińska J, Kiejza D, Ratkiewicz A, Piekutin J, Makarova K, et al. Oxidation of contaminants of emerging concern by combination of peracetic acid with iron ions and various types of light radiation – optimization, kinetics, removal efficiency and mechanism investigation. J Mol Liq. 2023;369: 120859. https://doi.org/10.1016/j.molliq.2022.120859.
7. Luukkonen T, Pehkonen SO. Peracids in water treatment: a critical review. Crit Rev Environ Sci Technol. 2017;47:1–39. https://doi.org/10.1080/10643389.2016.1272343.
8. da Silva WP, Carlos TD, Cavallini GS, Pereira DH. Peracetic acid: structural elucidation for applications in wastewater treatment. Water Res. 2020;168: 115143. https://doi.org/10.1016/j.watres.2019.115143.
9. Bawn CEH, Williamson JB. The oxidation of acetaldehyde in solution. Part II—Kinetics and mechanism of the formation of peracetic acid. Trans Faraday Soc. 1954;47:735–43. https://doi.org/10.1039/TF9514700735.
10. Kim J, Zhang T, Liu W, Du P, Dobson JT, Huang C-H. Advanced oxidation process with peracetic acid and Fe(II) for contaminant degradation. Environ Sci Technol. 2019;53:13312–22. https://doi.org/10.1021/acs.est.9b02991.
11. Sciscenko I, Vione D, Minella M. Infancy of peracetic acid activation by iron, a new Fenton-based process: A review. Heliyon. 2024;10: e27036. https://doi.org/10.1016/j.heliyon.2024.e27036.
12. Wang S, Wang H, Liu Y, Fu Y. Effective degradation of sulfamethoxazole with Fe2+-zeolite/peracetic acid. Sep Purif Technol. 2020;233: 115973. https://doi.org/10.1016/j.seppur.2019.115973.
13. APHA. Standard methods for the examination of water and wastewater. 23rd ed. American Public Health Association: Washington, D.C; 2017.
14. Chick H. An investigation of the laws of disinfection. J Hyg (Lond). 1908;8:92–158. https://doi.org/10.1017/S0022172400006987.
15. Daniel LA, Brandão CCS, Guimarães JR, Libânio M, de Luca SJ. Métodos alternativos de desinfecção da Água: processos de Desinfecção e desinfetantes alternativos na produção de água potável. 1st ed. Sao Carlos: RiMa Artes e textos; 2001.
16. Vosko SH, Wilk L, Nusair M. Accurate spin-dependent electron liquid correlation energies for local spin density calculations: a critical analysis. Can J Phys. 1980;58:1200–11. https://doi.org/10.1139/p80-159.
17. Lee C, Yang W, Parr RG. Development of the Colle-Salvetti correlation-energy formula into a functional of the electron density. Phys Rev B. 1988;37:785–9. https://doi.org/10.1103/PhysRevB.37.785.
18. Becke AD. Density-functional thermochemistry III the role of exact exchange. J Chem Phys. 1993;98:5648–52. https://doi.org/10.1063/1.464913.
19. Stephens PJ, Devlin FJ, Chabalowski CF, Frisch MJ. Ab initio calculation of vibrational absorption and circular dichroism spectra using density functional force fields. J Phys Chem. 1994;98:11623–7. https://doi.org/10.1021/j100096a001.
20. Ditchfield R, Hehre WJ, Pople JA. Self-consistent molecular-orbital methods. IX an extended gaussian-type basis for molecular-orbital studies of organic molecules. J Chem Phys. 1971;54:724–8. https://doi.org/10.1063/1.1674902.
21. Hehre WJ, Ditchfield R, Pople JA. Self — consistent molecular orbital methods xii further extensions of gaussian — type basis sets for use in molecular orbital studies of organic molecules. J Chem Phys. 1972;56:2257. https://doi.org/10.1063/1.1677527.
22. Hariharan PC, Pople JA. The influence of polarization functions on molecular orbital hydrogenation energies. Theor Chim Acta. 1973;28:213–22. https://doi.org/10.1007/BF00533485.
23. Marenich AV, Cramer CJ, Truhlar DG. Universal solvation model based on solute electron density and on a continuum model of the solvent defined by the bulk dielectric constant and atomic surface tensions. J Phys Chem B. 2009;113:6378–96. https://doi.org/10.1021/jp810292n.
24. Parr RG, Yang W. Density-functional theory of atoms and molecules. USA.: Oxford University Press; 1994.
25. Glendening ED, Landis CR, Weinhold F. Natural bond orbital methods. WIREs Comput Mol Sci. 2012;2:1–42. https://doi.org/10.1002/wcms.51.
26. Frisch MJ, Trucks GW, Schlegel HB, Scuseria GE, Robb MA, Cheeseman JR, et al. Gaussian 09 Revision D01. Wallingford CT: Gaussian Inc; 2009.

27. Dennigon R, Keith T, Millam J. 2009. Gauss View, Version 5. Semichem Inc., Shawnee Mission.;.
28. Pignatello JJ, Oliveros E, MacKay A. Advanced oxidation processes for organic contaminant destruction based on the fenton reaction and related chemistry. Crit Rev Environ Sci Technol. 2006;36:1–84. https://doi.org/10.1080/10643380500326564.
29. Ksibi M. Chemical oxidation with hydrogen peroxide for domestic wastewater treatment. Chem Eng J. 2006;119:161–5. https://doi.org/10.1016/j.cej.2006.03.022.
30. Schumann P. Peptidoglycan structure. Methods Microbiol. 2011;38:101–29. https://doi.org/10.1016/B978-0-12-387730-7.00005-X.
31. Vollmer W, Bertsche U. Murein (peptidoglycan) structure, architecture and biosynthesis in Escherichia coli. Biochim Biophys Acta - Biomembr. 2008;1778:1714–34. https://doi.org/10.1016/j.bbamem.2007.06.007.
32. Lopes Grotto CG, Gomes Colares CJ, Lima DR, Pereira DH, Teixeira do Vale A. Energy potential of biomass from two types of genetically improved rice husks in Brazil: a theoretical-experimental study. Biomass Bioenergy. 2020;142:105816. https://doi.org/10.1016/j.biombioe.2020.105816.
33. Costa AMF, de Aguiar Filho SQ, Santos TJ, Pereira DH. Theoretical insights about the possibility of removing Pb^{2+} and Hg^{2+} metal ions using adsorptive processes and matrices of carboxymethyl diethylaminoethyl cellulose and cellulose nitrate biopolymers. J Mol Liq. 2021;331:115730. https://doi.org/10.1016/j.molliq.2021.115730.
34. Santos TJ, Paggiaro J, Cabral Silva Pimentel HD, dos Santos Karla, Pereira A, Cavallini GS, Pereira DH. Computational study of the interaction of heavy metal ions, Cd(II), Hg(II), and Pb(II) on lignin matrices. J Mol Graph Model. 2022;111: 108080. https://doi.org/10.1016/j.jmgm.2021.108080.
35. Pereira DH, La PFA, Santiago RT, Garcia DR, Ramalho TC. New perspectives on the role of frontier molecular orbitals in the study of chemical reactivity: a review. Rev Virtual Química. 2016;8:425–53. https://doi.org/10.5935/1984-6835.20160032.
36. Chaúque BJM, Rott MB. Solar disinfection (SODIS) technologies as alternative for large-scale public drinking water supply: advances and challenges. Chemosphere. 2021;281: 130754. https://doi.org/10.1016/j.chemosphere.2021.130754.
37. Gabet A, Métivier H, de Brauer C, Mailhot G, Brigante M. Hydrogen peroxide and persulfate activation using UVA-UVB radiation: degradation of estrogenic compounds and application in sewage treatment plant waters. J Hazard Mater. 2021;405: 124693. https://doi.org/10.1016/j.jhazmat.2020.124693.
38. Nelson KL, Boehm AB, Davies-Colley RJ, Dodd MC, Kohn T, Linden KG, et al. Sunlight-mediated inactivation of health-relevant microorganisms in water: a review of mechanisms and modeling approaches. Environ Sci Process Impacts. 2018;20:1089–122. https://doi.org/10.1039/C8EM00047F.
39. Saravanan A, Kumar PS, Jeevanantham S, Karishma S, Kiruthika AR. Photocatalytic disinfection of micro-organisms: mechanisms and applications. Environ Technol Innov. 2021;24: 101909. https://doi.org/10.1016/j.eti.2021.101909.
40. Yang C, Sun W, Ao X. Bacterial inactivation, DNA damage, and faster ATP degradation induced by ultraviolet disinfection. Front Environ Sci Eng. 2020;14:13. https://doi.org/10.1007/s11783-019-1192-6.